Journal of The Electrochemical Society, **157** (11) B1731-B1739 (2010)
0013-4651/2010/157(11)/B1731/9/$28.00 © The Electrochemical Society

Progress Toward Accurate Through-Plane Ion Transport Resistance Measurement of Thin Solid Electrolytes

Kevin R. Cooper[*,z]

Scribner Associates Incorporated, Southern Pines, North Carolina 28387, USA

An instrument and procedure for evaluation of the through-plane ionic resistance and conductivity of polymer electrolyte membranes (PEMs) is presented. The approach facilitates rapid evaluation of bare, as-manufactured membranes over a wide range of temperatures and relative humidity conditions. The use of bare membrane is a key feature because a primary application is the characterization of the ionic conductivity of developmental materials for which testing a fuel cell is not practicable. Accurate evaluation of through-plane resistance and conductivity requires adjusting the measured high frequency resistance for nonmembrane ohmic contributions. Nonmembrane ohmic contributions, referred to in this work as the cell resistance, was determined by extrapolating to zero thickness a linear regression of the measured high frequency resistance vs membrane thickness. The cell resistance was a function of temperature and relative humidity. Using the through-plane resistance corrected for the cell resistance, the area specific resistance and conductivity of dispersion-cast Nafion NR-212 was observed to be the same in the through- and in-plane directions.
 [DOI: 10.1149/1.3481561]

Manuscript submitted February 25, 2010; revised manuscript received July 26, 2010. Published September 28, 2010. This was Paper 973 presented at the Vienna, Austria, Meeting of the Society, October 4–9, 2009.

Efforts are underway to develop polymer electrolyte membranes (PEMs) with high ionic (protonic) conductivity at elevated temperature and low humidity, e.g., 0.1 S/cm at 120°C, <50% relative humidity (RH). Such operating conditions are considered necessary for successful commercialization of PEM fuel cell power systems for transportation applications.[1-3] Target membrane conductivities at other conditions, such as at −20°C and room temperature, have also been established.

Although ionic conductivity is a keystone performance property, an accepted, easily implemented, and rapid test protocol and measurement system for evaluating this property of PEMs in the through-plane direction is generally absent.

Present approaches to measuring the resistance in thin ionomer films and membranes can be classified as either in- or through-plane, with the added distinction of being either two- or four-electrode. Four-electrode/four-terminal (Kelvin connection) methods are readily applied to in-plane measurement of bare membrane[4-10] wherein the cell configuration and specimen geometry advantageously permit a large cell constant and the placement of independent voltage-sense electrodes.

Because it is easily implemented, the in-plane approach is generally used and, therefore, the measured resistance and the reported conductivity values are for ion transport within the plane of the membrane, rather than in the more relevant through-plane direction. Anisotropy in membrane conductivity may be an intrinsic property of the ionomer or may result from processing. For example, there are anecdotal reports that the extruded perfluorosulfonic acid (PFSA) membrane exhibit anisotropic conductivity within the plane of the membrane. That is, the conductivity differs between the extrusion and transverse directions. In addition, anisotropic behavior may arise due to the presence of macroscopic or microscopic nonconductive support structures and/or skin effects. Thus, the potential for anisotropic behavior should be considered when interpreting in-plane resistivity and conductivity data and when comparing to through-plane measurements. Consideration of nonisotropic membrane properties such as conductivity is important because it may impact cell performance.

Through-plane membrane resistance is generally restricted to two-electrode and two- or four-terminal (Kelvin connection) setups. Through-plane measurements are limited to two electrodes because of the challenge associated with locating independent voltage-sense electrodes in a thin ionically conductive phase. Electrodes that are located in but do not influence the potential field in the membrane are required for a true four-electrode measurement.

Two-electrode measurements suffer from contributions that are not due to the membrane, such as contact and electrode resistance and electrode–electrolyte interfacial impedance (i.e., charge-transfer resistance and double-layer capacitance). Although the impedance spectroscopy technique can account for the latter, the former can only be ascertained via measurement of membranes of multiple thicknesses and/or stacks of membranes. Through-plane techniques are also more difficult to implement experimentally than in-plane techniques because the magnitude of the membrane resistance is small, ca. 0.1–10 Ω.

Through-plane membrane resistance is usually obtained from single-cell testing,[11-13] although approaches that use bare membrane have been reported.[14,15] For single-cell testing, considerable time and skill are required to reproducibly catalyze the membrane and then to assemble, break-in, and test a single cell. When extracting the membrane through-plane resistance from single-cell data, nonmembrane ohmic contributions, such as the electronic resistance of the flow field and gas diffusion media and contact resistances, should be accounted for.[13]

A method for rapid and reliable measurement of the through-plane resistance of a bare (noncatalyzed) membrane material over a broad range of temperature and humidity conditions is needed. The ability to use bare membrane test samples is a key requirement of the test system and measurement protocol because of the need to evaluate a large number of developmental membranes. Using a catalyzed membrane would significantly increase the time, cost, and complexity of the evaluation process, which is undesirable for developmental membranes for which electrode/bulk membrane interfacial chemistry and processing parameters are unknown. In addition, the system should be operable at elevated pressures, which is required for the evaluation of membranes at high RH at temperatures above the boiling point of water.

This work presents the status of a purpose-built test device and procedure for through-plane membrane resistance and conductivity measurement. The instrument and procedure achieves the aforementioned requirements, including the ability to rapidly evaluate bare, as-manufactured membranes over a wide range of temperatures and RH conditions: 30 to >120°C and dry to >95% RH. Custom application software provides fully automated control of the membrane temperature, dew point and therefore RH, and rapid RH cycling using a wet–dry gas mixing humidification system. The resistance of the membrane is determined using a four-terminal (Kelvin connection), two-electrode impedance spectroscopy measurement.

Recent developments include determination of the area specific

* Electrochemical Society Active Member.
z E-mail: kevin@scribner.com

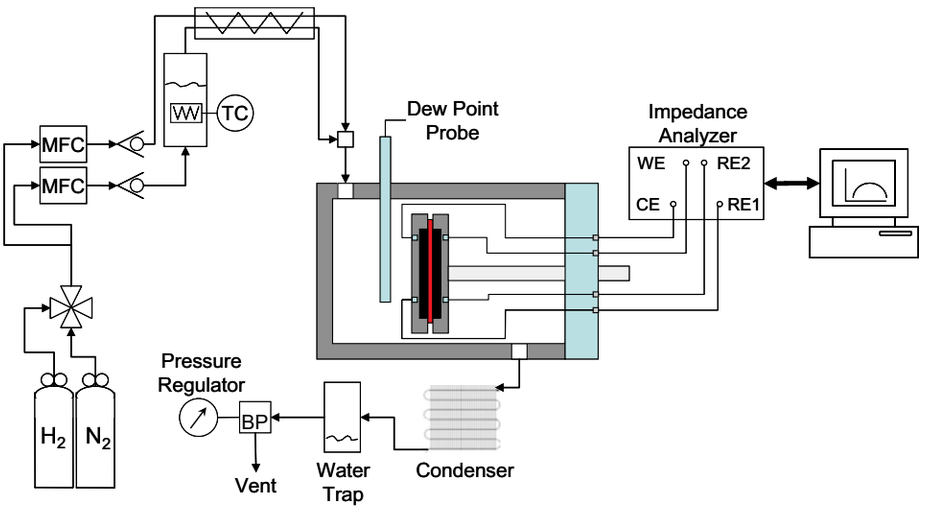

Figure 1. (Color online) Schematic of the major hardware components of the MTS, excluding the control electronics and DAQ system. System features: (*i*) Mass flow controllers for wet–dry gas mixing for rapid humidity changes and RH cycling; (*ii*) in situ dew point and temperature probes for real-time humidity measurement and RH calculation; and (*iii*) two-electrode/four-terminal (Kelvin connection) for through-plane resistance measurement via swept frequency impedance spectroscopy with an impedance analyzer.

cell resistance (ASR_{cell} in Ω cm^2), which must be accounted for to determine the membrane ASR and conductivity. Cell resistance (or ASR_{cell}) is a function of temperature and RH and must be determined for each condition, i.e., $ASR_{cell}(T,RH)$.

The status and results of the effort to develop a versatile, user-friendly membrane test system (MTS) and measurement protocol are presented.

Experimental

System for through-plane membrane resistance measurement.— The principal objective is to determine the through-plane resistance and conductivity of PEMs. In principle, the through-plane membrane conductivity (σ in S/cm) is determined from the membrane resistance (R in Ω), the thickness of the membrane (L in cm), and the cross-sectional area through which the current passes (A in cm^2)

$$\sigma = \frac{L}{RA} = \frac{I}{V}\frac{L}{A} \quad [1]$$

The requirements of such an MTS included the ability to accurately measure this material property over a range of temperature, humidity, and absolute pressure conditions. The main components of the MTS setup used in this work are illustrated in Fig. 1:

1. Wet–dry mixed gas handling system: humidifier, heated wet–dry gas mixing zone and transfer lines, two mass flow controllers, forced-air radiator, water collection tank, and back pressure regulator.
2. Test chamber and cell head: heated metal chamber with gas inlet and outlet, in situ gas dew point sensor (Vaisala, Inc.), cell head with integrated electrodes/specimen holder and specimen compression mechanism, and thermocouples for specimen temperature monitoring.
3. Control and data acquisition (DAQ): host computer-controlled custom electronics and application software for experimental setup, control, and DAQ.
4. Impedance measurement. Solartron Analytical 1260 frequency response analyzer (Ametek, Inc.) and ZPlot software (Scribner Associates, Inc.) for four-terminal impedance spectroscopy measurement.

The test cell head and electrode configuration is shown in Fig. 2. The test sample was fixed between opposing parallel electrodes under a compressive load.[16] Details of the sample assembly procedure are described below.

The offset electrode design shown in Fig. 2 took advantage of the fact that the current takes the path of least resistance (i.e., shortest distance) between the source electrodes. The current was therefore confined to the overlap region of the source electrodes because that is where the distance between the source electrodes was shortest. In addition, the platinum source electrode was equipotential because of its high conductivity. The membrane was thin and the distance between source electrodes was small, relative to the offset distance of the voltage-sense electrode from the source electrode that was located on the same side of the membrane. Because the current was confined to the region between the source electrodes overlap, there was no ohmic voltage drop in the membrane in the region where the voltage-sense electrodes were located. The voltage-sense electrode measured the same voltage as the source electrode that was located across the membrane from it.

Test procedure.— The test procedure for the through-plane resistance measurement consists of measuring the sample thickness, assembling it into test fixture, conditioning the membrane at the desired test temperature and RH, and obtaining impedance of the sample throughout a defined RH cycle. These are described further below; analysis of the impedance data is discussed in the Results and Discussion section.

Sample and cell assembly.— Membranes tested in this study included as-manufactured commercial extruded Nafion N11X series and cast Nafion NR-212 material with 1100 equivalent weight (EW), as well as composite membranes consisting of a PFSA-based proton-conducting phase (EW unknown) supported by an expanded poly(tetrafluoroethylene) reinforcement layer.

Membrane sample (3.0×1.0 cm) thickness was measured at five locations with a high precision, calibrated film thickness gauge (Brunswick Instruments, Inc. Film Thickness Measurement System-3, contact pressure = 15.17 kPa or 2.2 psi) at ambient conditions ($\sim$22°C, 50% RH). The mean thickness (L) was used in the calculation of the through-plane conductivity.

The membrane was compressed between gas diffusion electrode (GDE) media (E-TEK ELAT GDE 140-HT) attached to solid platinum backing electrodes with conductive carbon paint. Porous gas diffusion media in direct contact with the membrane facilitated gas-phase diffusion of water vapor to and from the membrane surface, thus permitting rapid changes in the hydration state of the thin membrane sample. The diffusion coefficient of water vapor in air was 0.239 cm^2/s,[17] whereas it was 10^{-6}–10^{-5} cm^2/s in Nafion, depending on temperature and water activity.[4,18-21] Therefore, by making available water vapor at the surface of both sides of the membrane via gas-phase transport with the porous backing media, the much slower diffusive transport of water within the membrane only had to occur over the much small distance, that is, half of the membrane

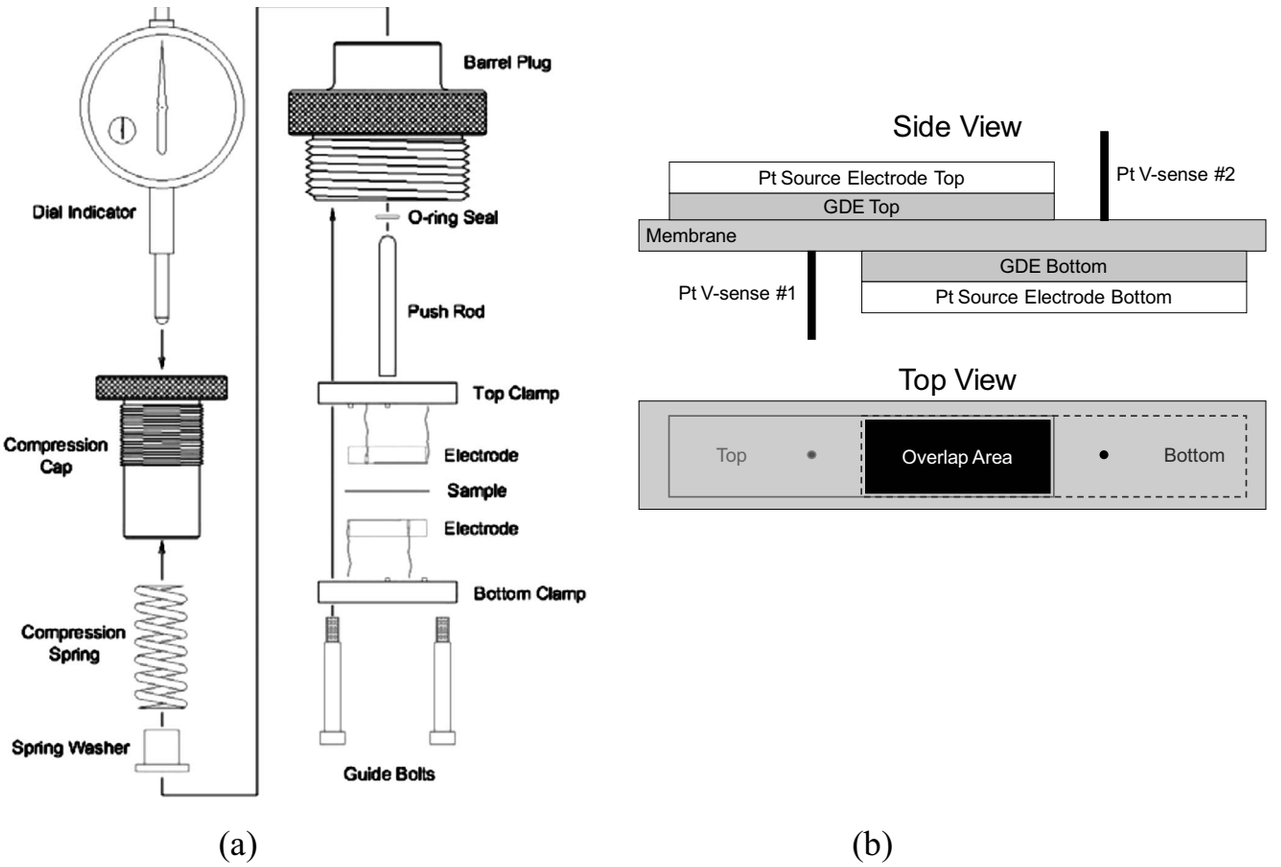

Figure 2. (a) Illustration of through-plane resistance measurement test system cell head and (b) detail of electrode configuration. GDE is composed of platinum catalyst-coated carbon cloth having a platinum catalyst layer on one side.

thickness. The use of a solid metal electrode as the contact layer with the membrane is not practical because of the difficulty in controlling the membrane water content.

Repeatable sample compressive loading to 2.151 ± 0.017 MPa (310 ± 2.5 psi) was achieved using a calibrated force spring and displacement indicator dial. Because the membrane sample was spring loaded, it was subject to fixed compression and was not constrained from swelling or shrinking in the through-thickness direction. Calculations reveal that there was negligible change in the compressive load as a result of changes in membrane thickness during testing. That is, by design, the change in membrane thickness and any corresponding spring compression was very small relative to the overall spring compression.

Test conditions.— Samples were tested over a wide range of temperature and humidity conditions: 30–120°C and dry to 100% RH. However, most testing to date followed the following procedure or a close variant of it. The sample was conditioned 2 h at 70% RH followed by stepping through the RH cycle: 70 to 20 to 90% at 10% intervals followed by 95%, with a 15 min duration at each RH before measurement of the membrane resistance. This RH cycle is typically performed at three temperature/pressure conditions, as shown in Table I.

A total dry gas flow rate of 500 sccm facilitated in attaining a steady-state RH within 2 min after a step change in the wet–dry gas ratio, i.e., a change in RH. Tests were conducted with either nitrogen or hydrogen with no difference in the high frequency impedance intercept. This observation was consistent with the notion that the high frequency impedance response was dominated by the electronic and ionic transport resistances with negligible contribution from the electrochemical charge-transfer or diffusion-transport processes.

Table I. General test conditions.

Temperature (°C)	30	80	120
Pressure (kPa_a)	100	100	230

Impedance measurement.— After conditioning the membrane for 15 min at a given RH, a voltage-controlled, swept frequency impedance spectroscopy measurement was performed using a commercial frequency response analyzer (10 mV_{ac} at 0 V_{dc}, 2 MHz–1 Hz, and 10 steps/decade). As discussed below, impedance spectra were fitted with an equivalent circuit model to determine the high frequency intercept.

Results and Discussion

Environmental control system performance.— The MTS environmental control system facilitates rapid changes in the humidity level of the test chamber, from dry to saturated (or supersaturated), as well as the operation over a wide range of test temperatures. The ability to rapidly change humidity level, and therefore RH, was deemed important for the characterization of membrane resistance and conductivity as a function of RH within a reasonable amount of time, e.g., <8 h. The ability to operate over a wide temperature range is important because of the requirement that the membrane resistance be characterized over a range of temperatures.

A typical RH cycle at 80°C is shown in Fig. 3. The wet–dry gas mixing of the MTS means that the humidifier temperature stays constant, whereas the proportions of wet and dry gases are changed to obtain the desired dew point and RH. The RH cycle shown here is typical of the aforementioned testing procedure. Each RH step lasted

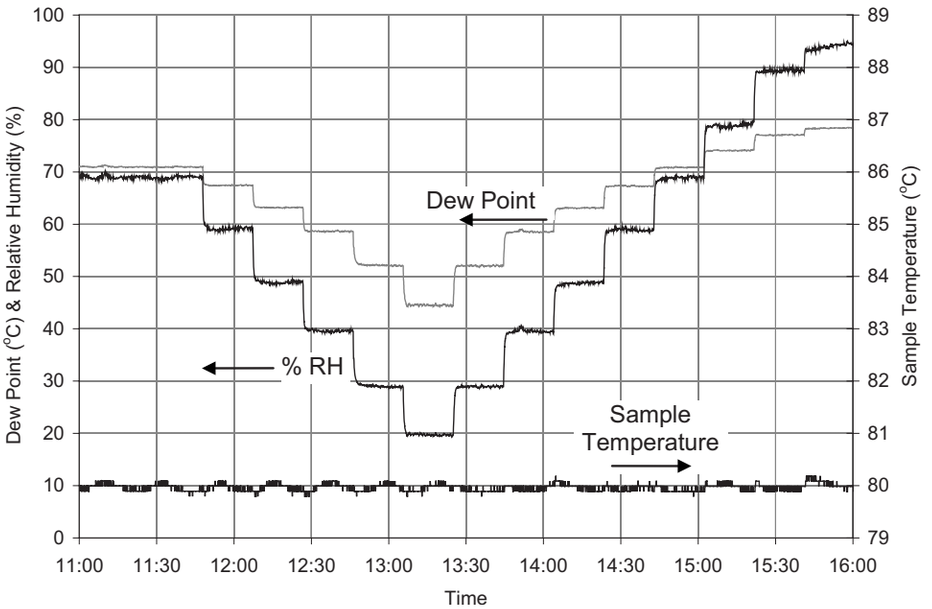

Figure 3. Typical temperature, dew point, and RH data for membrane testing at 80°C. Rapid change in dew point and RH achieved with the wet–dry mixing humidification system. Sample temperature was constant at 80 ± 0.2°C.

15 min plus the time required to make the impedance measurement. For each RH step, the new dew point and RH are established within ~1 min of the change in the wet–dry mix. The sample temperature was constant throughout the test at 80 ± 0.2°C.

As indicated elsewhere in this work, for ionomers and membranes (such as PFSAs) whose resistance is a strong function of water content, reproducible environmental conditions are essential for reproducible membrane resistance data. Table II summarizes the day-to-day performance of the environmental control system. Mean ($\bar{X}$) and standard deviation (s) of the RH at 30 and 80°C across multiple days of operation are reported. For the preponderance of temperature–RH combinations, mean RH values were consistent within 1% RH of the nominal or target value. The exception was the high humidity region at 30°C in which the MTS was consistently within ~2% RH of the target value.

Environmental performance data at 120°C were excluded because the in situ humidity probe does not operate at dew point above 100°C (i.e., ~30% RH at 120°C). Thus, real-time measurement of the RH at 120°C is limited to the low RH regime. For this, a water mass balance study was used to calibrate the MTS humidification system at this temperature.

Time dependence of membrane hydration.— To examine the time dependence of the membrane to a change in humidity, experiments were performed in which the sample was conditioned for 2 h at 30% RH before rapidly stepping to 80% RH. Impedance spectra were obtained at the low RH condition just before stepping to high RH and then successively at the 80% RH condition. Five replicate experiments were performed to gauge the reproducibility of the through-plane method.

The results are shown in Fig. 4. The solid symbols (■) reflect the mean ASR at time t after the step to 80% RH normalized to the ASR observed at t = 62.5 min. This latter value is taken as the near-equilibrium membrane resistance. The open symbols show the membrane ASR for the replicate tests. The membrane resistance at 30% RH, indicated at t = 0, was an order of magnitude higher than the near-equilibrium value at 80% RH, i.e., $ASR_{30\%\ RH}$ = 201 ± 27 mΩ cm^2 vs $ASR_{80\%\ RH}$ = 20 ± 2 mΩ cm^2. It took ~1 min for the RH to stabilize at 80% after the step was initiated at t = 0.

The results of these tests indicate that within 15 min, the resistance of a thin (18 μm) PFSA-based membrane such as the one used here is within 10% of the near-equilibrium value observed after extended exposure. This test imposed a significantly greater change in RH than what is typically used when characterizing the membrane. The usual RH step size was 10–20% RH, whereas in these tests, the RH changed from 30 to 80%. Because the membrane went from a relatively dry to humid condition, the change in water content of the membrane is expected to be large compared to a small change in RH. Thus, the membrane achieves near-equilibrium hydration, and therefore resistance, within 15 min when subjected to a smaller change in RH, as is used in the general procedure.

Thicker membranes are expected to respond more slowly than

Table II. Reproducibility of the environmental control system across N days at 30 and 80°C (s = standard deviation).

	30°C (N = 15)		80°C (N = 11)	
Nominal % RH	$\bar{X}_{1s}$	Difference from nominal % RH	$\bar{X}_{1s}$	Difference from nominal % RH
20	$20.5_{0.29}$	0.5	$19.7_{0.22}$	−0.3
30	$30.7_{0.38}$	0.7	$28.9_{0.24}$	−1.1
40	$40.7_{0.48}$	0.7	$39.5_{0.33}$	−0.5
50	$50.5_{0.54}$	0.5	$48.9_{0.36}$	−1.1
60	$59.8_{0.74}$	−0.2	$59.2_{0.37}$	−0.8
70	$69.3_{0.87}$	−0.7	$69.2_{0.43}$	−0.8
80	$78.6_{0.97}$	−1.4	$79.6_{0.56}$	−0.4
90	$88.5_{1.00}$	−1.5	$90.3_{0.61}$	0.3
95	$92.8_{1.02}$	−2.2	$94.7_{0.48}$	−0.3

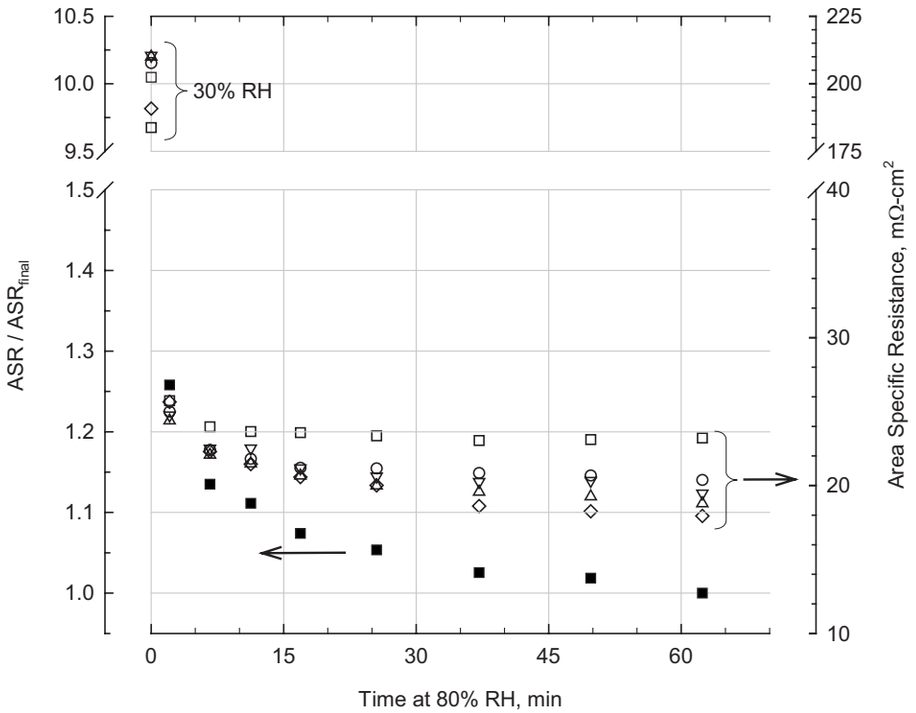

Figure 4. Membrane through-plane resistance as a function of time t on stepping from 30 to 80% RH at 80°C. Data at $t = 0$ were acquired after conditioning the sample for 2 h at 30% RH. The ASR normalized to the ASR at 62.5 min (ASR_{final}) is shown by the filled symbols (■). ASR vs time for five replicates (unique samples from the same production lot) is shown by the open symbols. Membrane: 18 μm PFSA-based (EW unknown). Within ~15 min, the membrane resistance differed by less than 10% of the near-equilibrium value.

thin material to a change in RH and, therefore, longer hold times might be required to achieve equilibrium behavior for the former. In addition, other ionomer chemistries may exhibit different hydration kinetics and time–humidity response with respect to conductivity and other properties.

Reproducibility.— The results shown in Fig. 4 also demonstrate the reproducibility of the through-plane membrane test method used in this work. Nominally identical samples taken from the same production lot were used, as were the test conditions. Membrane thickness was 19.0 ± 1.3 μm.

The membrane resistance measurement was reasonably reproducible from sample to sample. However, one data set (□) deviated from the other four sets. There are insufficient data to ascertain if this data set is a statistical outlier.

One potential source of variability in resistance is variations in the test conditions, in particular, temperature and RH. The conductivity of the PFSA membrane is a strong function of RH and is to a lesser degree temperature. For both environmental variables, an increase in their value results in an increase in conductivity and decrease in resistance.

The correlation between the measured resistance and the RH at the time of measurement was quantitatively evaluated. Tests were at the same nominal test condition, i.e., 80°C and 80% RH. The correlation coefficient R^2 was 0.49, indicating that approximately half of the run-to-run variability in resistance for the data shown in Fig. 4 is attributable to very small differences in RH. The range of RH was less than 2% in this analysis. The analysis also revealed the very strong dependence of the resistance on RH: ~1.3 mΩ cm^2 per percent change in RH for the PFSA membrane used here.

RH is affected by the absolute humidity (represented here by dew point) and temperature. The source of variability in RH was due to the run-to-run variation in dew point ($R^2 = 0.39$) and temperature ($R^2 = 0.46$). The results highlight the very strong sensitivity of the PFSA membrane to environmental conditions, in particular, RH.

Analysis of resistance data for membrane ASR and conductivity.— Impedance spectra acquired at RH from 20 to 95% at 80°C are shown in Fig. 5, wherein Bode and Nyquist (complex plane) plots are shown for completeness. The membrane was a thin (18 μm) PFSA-based material. Both the low and high frequency impedances exhibit humidity dependence. The low frequency impedance is the sum of the ohmic resistance and the charge-transfer impedance of the two electrodes. There is no apparent evidence of mass transport impedance in these results. The portion of the impedance spectra that is of interest is the high frequency region because that is indicative of the membrane resistance.

The high frequency intercept is the sum of a series of ohmic resistances. Although dominated by the membrane resistance, in a two-electrode/four-terminal measurement, there are nonmembrane contributions to the high frequency impedance. These include small but non-negligible contributions of the electronic resistance of the gas diffusion media, Pt-backing electrode, and the contact resistance between the two. In addition, there is an ohmic impedance at the interface between the electrode and electrolyte, which also contributes to the high frequency impedance.[22,23] Pivovar and Kim[23] describe the membrane–electrode interfacial resistance as arising from the contact between the solid electrolyte and electrode layers. This interfacial resistance was 10–60 mΩ cm^2, depending on the membrane type (Nafion, recast Nafion, and hydrocarbon) and relatively independent of temperature; the effect of RH on the membrane–electrode interfacial resistance was not investigated.[23] For the purposes of this work, we lump all nonmembrane ohmic contributions to the high frequency intercept into a factor we call the cell resistance, $R_{cell}(\Omega)$. Because resistance values are typically normalized for the active area, we define a cell ASR to account for all nonmembrane ohmic resistances, ASR_{cell} (Ω cm^2). R_{cell} (or ASR_{cell}) itself exhibits temperature and RH dependence and therefore must be determined for each test condition, i.e., each temperature–RH condition.

The first step toward determining the membrane resistance is to analyze the impedance spectra to determine the high frequency intercept (R_{HF}). This analysis was performed using least-squares fitting of the impedance spectra data to the equivalent circuit model, as shown in Fig. 6 using ZView software (Scribner Associates, Inc).

The uncorrected ASR ($ASR_{uncorrected}$) is the product of R_{HF} and the effective area ($A_{effective}$ in cm^2)

$$ASR_{uncorrected}(T,\mathrm{RH}) = R_{HF}(T,RH) \times A_{effective} \quad (\Omega\ \mathrm{cm}^2) \quad [2]$$

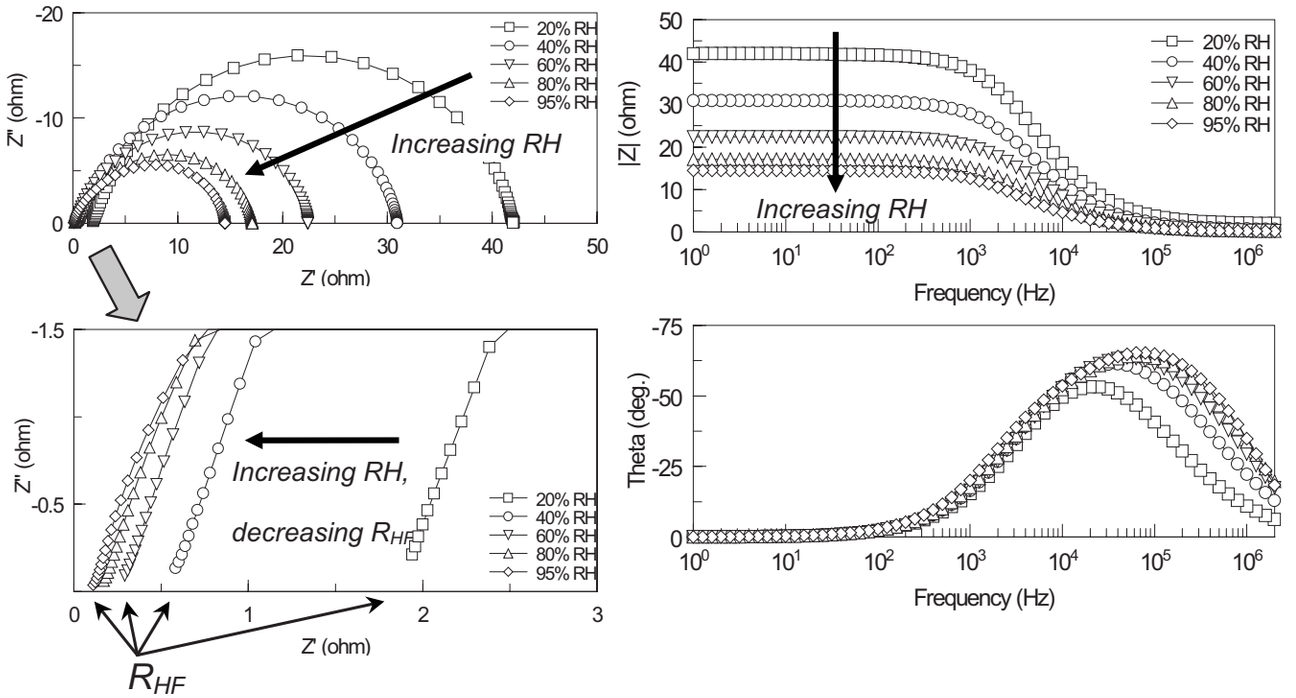

Figure 5. Impedance spectra for a PFSA membrane at 80°C for RH ranging from 20 to 95%. The total ohmic resistance, which is the sum of the membrane and nonmembrane ohmic resistances of the cell, is given by the high frequency intercept (R_{HF}). R_{HF} is determined from an equivalent circuit model fit of the impedance spectra using the model shown in Fig. 6. Nominal active area = 0.5 cm^2.

The effective sample area was determined post-test by the analysis of digital images of the sample.

Accurate determination of the membrane ASR and conductivity requires correcting the as-measured ASR for the nonmembrane ohmic resistances that contribute to the measured high frequency resistance. The membrane ASR is the difference between the as-measured, uncorrected ASR and the cell ASR

$$\mathrm{ASR}_{\mathrm{membrane}}(T,\mathrm{RH}) = \mathrm{ASR}_{\mathrm{uncorrected}}(T,\mathrm{RH}) - \mathrm{ASR}_{\mathrm{cell}}(T,\mathrm{RH}) \quad (\Omega\ \mathrm{cm}^2) \qquad [3]$$

All terms in Eq. 2 are a function of the test conditions, i.e., temperature and humidity. Membrane conductivity ($\sigma_{\mathrm{membrane}}$) (in S/cm) is given by

$$\sigma_{\mathrm{membrane}}(T,\mathrm{RH}) = \frac{L}{\mathrm{ASR}_{\mathrm{membrane}}(T,\mathrm{RH})} \quad (\mathrm{S/cm}) \qquad [4]$$

where L (cm) is the thickness of the membrane. In practice, membrane thickness is measured at ambient conditions before testing. For membranes that are subject to dimensional changes as a result of hydration or other causes of swelling, an improved method would be to determine the membrane thickness at each test condition. Thus, a caveat with conductivity values reported here is that they are based on the membrane thickness determined under ambient temperature and RH.

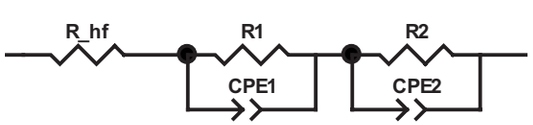

Figure 6. Equivalent circuit model for analysis of impedance spectra for determination of the high frequency intercept (R_{HF}). CPE is constant phase element. In some cases, a series inductor was included in the model to account for high frequency inductance artifact in the data.

In a process similar to that used by Alberti and co-workers,[14] the cell resistance ($\mathrm{ASR}_{\mathrm{cell}}$) was determined by extrapolation to the theoretical zero membrane thickness via linear regression of the as-measured, uncorrected ASR value vs membrane thickness data. Typical data for one PFSA membrane system are shown in Fig. 7. Data acquired from replicate measurements of at least three membrane thicknesses of nominally identical ionomers were used in this analysis. This was done for each temperature and RH condition.

Two different sets of PFSA-based membrane materials were used to determine two $\mathrm{ASR}_{\mathrm{cell}}(T,\mathrm{RH})$ values. Mean $\mathrm{ASR}_{\mathrm{cell}}$ values as a function of temperature and RH are shown in Fig. 8. There was reasonable agreement in the estimated cell resistance for comparable RH conditions. That is, the cell resistance was generally within 30% each other for a given temperature and RH.

The coefficient of determination (R^2) for the linear regression of $\mathrm{ASR}_{\mathrm{HF}}$ vs thickness ranged from 94.3 to 98.8%. The relatively high R^2 indicates that there was a very strong positive correlation between the measured resistance and thickness, as one would expect if there was no significant error or variability in the data.

The primary assumption in this analysis is that the intrinsic conductivity of Nafion (or other ionomers) of a given EW or ion exchange capacity is independent of thickness. A justification that this assumption is valid, at least within the accuracy achieved in this work, is provided by the very high correlation coefficients ($R^2 \sim 0.94$ to 0.99) observed for all linear regression fits of the measured resistance vs thickness for the membranes used in this work. The assumption of thickness-independent conductivity may not hold for other membrane chemistries, manufacturing methods, and thermomechanical processing history.

Furthermore, this analysis assumes that the variability in conductivity of samples from different production batches is small relative to the overall measured resistance. Lastly, this analysis assumes that at a given test condition, e.g., temperature and RH, the cell resistance is constant from test sample to test sample.

It is worth examining the magnitude of the nonmembrane ohmic

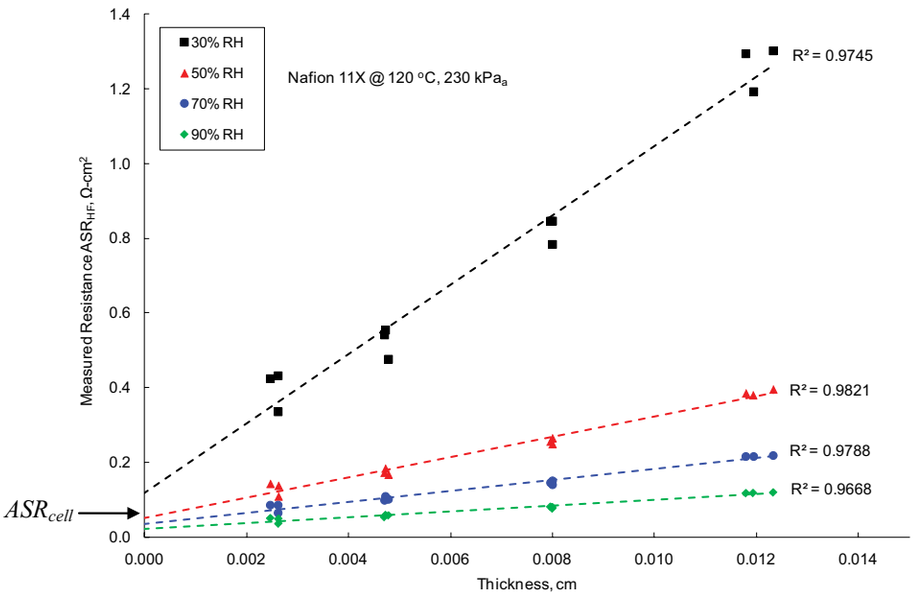

Figure 7. (Color online) Cell resistance $ASR_{cell}(T,RH)$ is the intercept of a plot of the area-normalized high frequency resistance vs membrane thickness. Triplicate measurements for nominally identical commercial PFSA membranes of four thicknesses were used (1100 EW Nafion 111, 112, 1135, and 115). Data at 120°C 230 kPa at the indicated RH.

resistance relative to the resistance of the membrane. Figure 9 shows the cell resistance normalized by the membrane resistance for three membranes (Nafion 111, 1135, and 117) at 120°C for a range of RHs. For the two sets of membranes used in this study, the 120°C condition represented the worst case because the membrane resistance was the lowest, whereas the cell resistance was not a strong function of temperature (see Fig. 8).

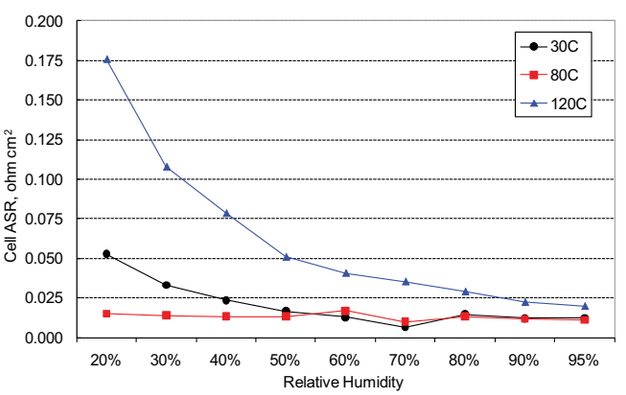

Figure 8. (Color online) ASR_{cell} as a function of temperature and RH as determined for two different sets of PFSA-based membranes described previously.

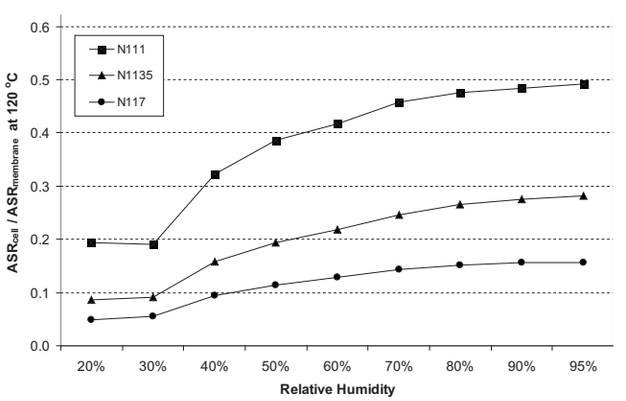

Figure 9. Ratio of the cell to the membrane ASR for Nafion 111, 1135, and 117 at 120°C.

Of course, the cell resistance (ASR_{cell}) is a larger fraction of the membrane resistance for thin membranes than for thick membranes. For nominally 25 μm (0.001 in.) thick Nafion 111, the cell resistance was nearly one-fifth of the membrane resistance at 20% RH and approached half its value at high RH. For the much thicker Nafion 117 (nominally 178 μm or 0.007 in. thick), the cell resistance was 5% of the membrane resistance at low RH and only 15% near water vapor saturation.

These data also illustrate that the cell resistance is a larger fraction of the membrane resistance at high RH than at low RH. This indicates that the membrane resistance decreases more rapidly with increasing RH than the cell resistance, reflected in the fact that the ratio of membrane resistance at 20 and 95% RH is ~20 to 30, whereas it was ~5 to 12 for ASR_{cell} at the same RHs.

These results show that, in general, accounting (or not accounting) for the cell resistance has a greater influence on the calculated membrane ASR and conductivity for thin membranes at high RH conditions. Also demonstrated by the data is that when given thin membranes at high RH, not accounting for the cell resistance can significantly alter the apparent membrane resistance and conductivity. The error that would result from not accounting for the cell resistance could approach 25–35% under some conditions. In contrast, at low humidity and/or for thick membranes, correction for the cell resistance alters the calculated membrane ASR and conductivity by 5–20%.

Challenges.— The primary challenge with the through-plane membrane resistance measurement method described is that to obtain accurate membrane ASR data, it may be necessary to account for the nonmembrane ohmic resistance that contributes to the measured high frequency resistance in a two-electrode measurement. That is, an accurate membrane ASR determination should include a correction for the presence of nonmembrane-derived ohmic sources. This is especially true for thin membranes where, as shown in Fig. 9, under some conditions, the contribution of the nonmembrane-sourced cell resistance can approach that of the membrane itself. Although at low RH, the cell resistance is small relative to the membrane resistance (e.g., $ASR_{cell}/ASR_{membrane} < 0.1$), at high RH, the cell resistance can be a significant portion of the membrane

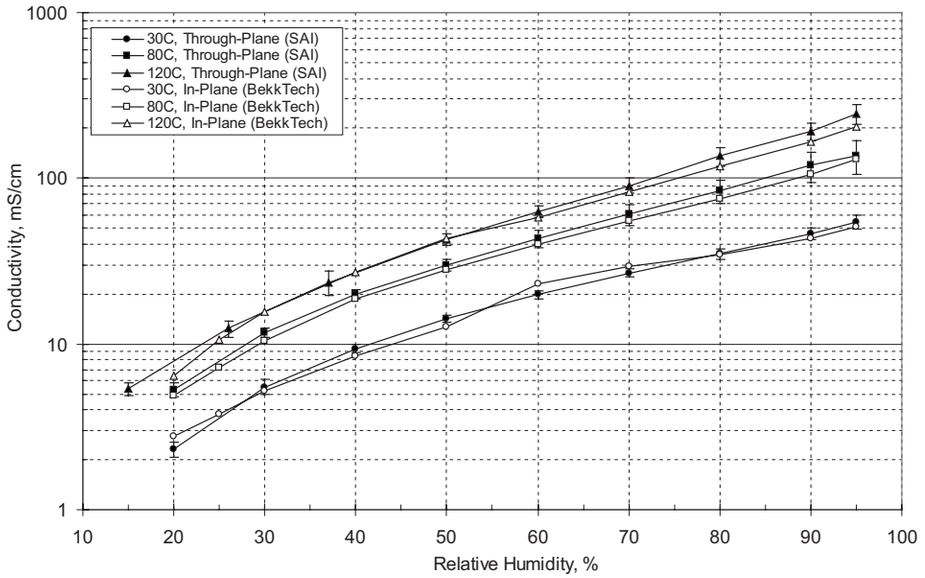

Figure 10. Comparison of the through-plane (filled symbols) and in-plane (open symbols) membrane conductivities of dispersion-cast Nafion NR-212 at 30, 80, and 120°C. Conductivity is based on thickness measured at ambient temperature and humidity. Through-plane conductivity values calculated from Eq. 4 using $ASR_{membrane}$ (i.e., corrected for ASR_{cell}). Mean and range are shown for through-plane data ($N_{30°C} = 7$, $N_{80°C} = 10$, and $N_{120°C} = 5$). In-plane data courtesy of BekkTech LLC.

resistance (e.g., $ASR_{cell}/ASR_{membrane} \sim 0.5$). Omission of the correction factor can lead to overestimation of the membrane resistance.

The challenge with the need to correct the measured resistance for the cell resistance is practical. To effectively perform the analysis method described here involves characterization of the resistance of a set of at least three membranes of different thicknesses of nominally identical intrinsic conductivity. In practice, this may present a challenge for membranes that are at the research and development stage, where fabrication of membranes of controlled, different thicknesses may be a challenge.

A viable alternative approach described by Alberti et al.[14] encompasses measuring the resistance of stacks of membrane to achieve the necessary thickness variation required to determine the cell resistance. An additional ohmic contribution from the intermembrane contact resistance is introduced with this method.

The cell resistance should be determined for each type of membrane. This is because the membrane–electrode interfacial resistance is a significant component of the cell resistance. The interfacial resistance may be a strong function of the membrane composition and microstructure, including ionomer chemistry and/or presence of additives or support material, as well as physical and mechanical properties (e.g., swellability, plasticity, and hardness of the membrane). As such, the interfacial resistance and therefore the cell resistance may differ for each membrane. Because accurate determination of the membrane resistance and conductivity requires accounting for the presence of the cell resistance, in principle, it should be determined for each type of membrane.

Comparison of in- and through-plane conductivities of Nafion.— Figure 10 summarizes the conductivity of Nafion NR-212 at three temperatures determined by the through-plane method described in this work and an in-plane method. In-plane results are courtesy of BekkTech LLC and are based on a four-electrode dc measurement. Through-plane data were corrected for the cell resistance via the approach detailed above and in both cases the conductivity was calculated using the membrane thickness measured at ambient temperature and RH (~22°C and 30–50% RH at the author's location).

Very strong agreement was observed in the membrane ASR and conductivity obtained by the two methods. The strong similarity in results across the broad range of test conditions is perhaps surprising, given the historical tendency for significant differences in reported conductivities for Nafion. Demonstration of the significant variability in the reported conductivity of Nafion 117 at 30°C is shown in Fig. 11. In some cases, the range in the reported conductivity varied by an order of magnitude. For this data summary, at least, there is no obvious consistent difference between in- and through-plane data. Indeed, the through-plane bound the in-plane data, with the values in this work close to the majority of the in-plane conductivity results.

As of now, there is no consensus among the community as to whether the conductivity of Nafion is anisotropic. Subsequently, it is not known whether systematic differences in the in- and through-plane conductivities of Nafion membranes can be expected.

Gardner and Anantaraman[24] reported that the conductivity of Nafion 117 is anisotropic after finding that the in-plane conductivity was more than 3 times greater than the through-plane conductivity. Ma et al.[9] also reported that the in-plane conductivity of Nafion was 2.5–5 times greater compared to the through-plane conductivity. The authors note, however, that the anisotropy was the result of the through-plane samples being subjected to extreme hot-pressing conditions (up to 117 MPa or 17,000 psi at 150°C), resulting in a microstructural modification to the test sample. In fact, Ma et al.[9] note that for samples not subjected to the compressive load, the conductivity was essentially the same for the two orientations.

Papers on the anisotropic conductivity of Nafion have been disputed by several studies. For example, Fedkiw et al.[25] reported that in-plane and through-thickness conductivity of Nafion 112 and 117 were essentially the same. Silva and co-workers[26] thoroughly investigated the orientation dependence of Nafion membrane conductivity and concluded that its conductivity is the same in the through- and in-plane orientations. Silva et al. concluded that Nafion membranes exhibit isotropic behavior; the in- and through-plane conductivities were equivalent when the hydration level (water content of the membrane) was identical.

In a careful analysis of the published literature, Silva and co-workers[26] noted that much of the discrepancy surrounding the papers on the conductivity of Nafion may be attributed to some or a combination of the following: (*i*) differences in handling and/or treatment of samples before testing; (*ii*) differences in measurement method, including two- and four-terminal and dc or ac impedance measurement approaches, which require different data treatment; and (*iii*) different experimental procedures and conditions including equilibration time, exposure conditions such as immersed in water vs water vapor, saturated gas exposure, etc.

Discrepancies between reported conductivities may in part result from inherent polymer batch processing methods and partly because

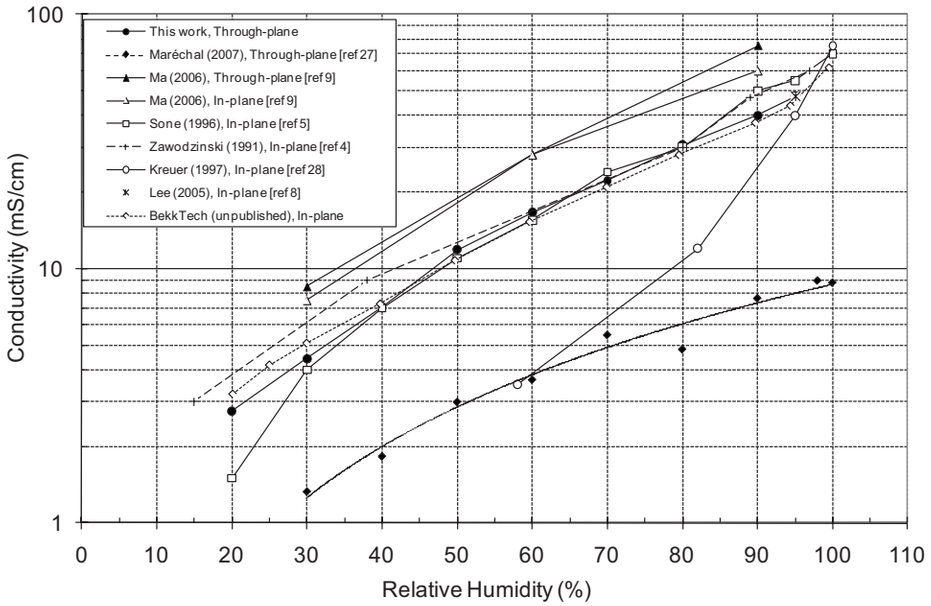

Figure 11. Reported Nafion 117 conductivities at 30°C vary by up to an order of magnitude. Data from this work were calculated from Eq. 4 using $ASR_{membrane}$ (i.e., corrected for ASR_{cell}). Data at 100% RH are for water vapor-saturated conditions and are not immersed in liquid water or other aqueous solution.

of differences in membrane processing (thermal, mechanical, and/or chemical processing history) resulting in differences in membrane morphology, particularly in the hydrated state.

Conclusions

A device and measurement procedure was developed for through-plane resistance and conductivity characterization of PEMs at temperatures and RHs that are of interest for fuel cell applications. As-manufactured, noncatalyzed membrane specimens can be tested, which is beneficial for the increased sample throughput and for the analysis of developmental membranes for which single-cell testing may not be practicable. Although more challenging to perform than the in-plane method, the through-plane approach has the advantage that the measured parameter is for the orientation that is relevant for fuel cell applications.

For accurate ASR and conductivity, the measured high frequency resistance should be corrected for the small, nonmembrane ohmic resistance, referred to here as the cell resistance or cell ASR. The nonmembrane ohmic contribution to the high frequency resistance was determined by extrapolating to zero thickness a linear regression of the measured high frequency resistance vs membrane thickness. The cell resistance was a function of temperature and RH. After correcting for the nonmembrane cell resistance, the ASR and the conductivity of as-received dispersion-cast Nafion NR-212 was essentially the same in the through- and in-plane directions for the environmental conditions examined.

Acknowledgments

This work was supported by the U.S. Department of Energy through the University of Central Florida. In-plane membrane resistance and conductivity data are courtesy of Tim Bekkedahl, BekkTech LLC. Nafion is a registered trademark of E. I. DuPont de Nemours and Co.

Scribner Associates, Inc. assisted in meeting the publication costs of this article.

References

1. U.S. Department of Energy, Hydrogen, Fuel Cells & Infrastructure Technologies Program Multi-Year Research, Development and Demonstration Plan (2005).
2. H. A. Gasteiger and M. F. Mathias, in *Proton Conducting Membrane Fuel Cells III*, M. Murthy, T. F. Fuller, J. W. Van Zee, and S. Gottesfeld, Editors, PV 2002-31, p. 1, The Electrochemical Society Proceedings Series, Pennington, NJ (2005).
3. M. F. Mathias, R. Makharia, H. A. Gasteiger, J. J. Conley, T. F. Fuller, C. J. Gittleman, S. S. Kocha, D. P. Miller, C. K. Mittelsteadt, T. Xie, et al., *Electrochem. Soc. Interface*, **14**, 24 (2005).
4. T. A. Zawodzinski, M. Neeman, L. O. Sillerud, and S. Gottesfeld, *J. Phys. Chem.*, **95**, 6040 (1991).
5. Y. Sone, P. Ekdunge, and D. Simonsson, *J. Electrochem. Soc.*, **143**, 1254 (1996).
6. J. J. Fontanella, M. C. Wintersgill, R. S. Chen, Y. Wu, and S. G. Greenbaum, *Electrochim. Acta*, **40**, 2321 (1995).
7. P. C. Rieke and N. E. Vanderborgh, *J. Membr. Sci.*, **32**, 313 (1987).
8. C. H. Lee, H. B. Park, Y. M. Lee, and R. D. Lee, *Ind. Eng. Chem. Res.*, **44**, 7617 (2005).
9. S. Ma, Z. Siroma, and H. Tanaka, *J. Electrochem. Soc.*, **153**, A2274 (2006).
10. B. D. Cahan and J. S. Wainright, *J. Electrochem. Soc.*, **140**, L185 (1993).
11. M. V. Williams, H. R. Kunz, and J. M. Fenton, *J. Electrochem. Soc.*, **152**, A635 (2005).
12. Z. Xie, C. Song, B. Andreaus, T. Navessin, Z. Shi, J. Zhang, and S. Holdcroft, *J. Electrochem. Soc.*, **153**, E173 (2006).
13. R. Makharia, M. F. Mathias, and D. R. Baker, *J. Electrochem. Soc.*, **152**, A970 (2005).
14. G. Alberti, M. Casciola, L. Massinelli, and B. Bauer, *J. Membr. Sci.*, **185**, 73 (2001).
15. M. Watanabe, H. Igarashi, I. Uchida, and F. Hirasawa, *J. Electroanal. Chem.*, **399**, 239 (1995).
16. K. R. Cooper and L. L. Scribner, U.S. Pat. 7,652,479 B2 (2010).
17. *CRC Handbook of Chemistry and Physics*, 70th ed., R. C. Weast and D. R. Lides, Editors, CRC Press, Boca Raton, FL (1990).
18. K. A. Mauritz and R. B. Moore, *Chem. Rev. (Washington, D.C.)*, **104**, 4535 (2004).
19. D. T. Hallinan, Jr. and Y. A. Elabd, *J. Phys. Chem. B*, **111**, 13221 (2007).
20. P. Majsztrik, A. Bocarsly, and J. Benziger, *J. Phys. Chem. B*, **112**, 16280 (2008).
21. J. T. A. Zawodzinski, T. E. Springer, J. Davey, R. Jestel, C. Lopez, J. Valerio, and S. Gottesfeld, *J. Electrochem. Soc.*, **140**, 1981 (1993).
22. R. Jiang, C. K. Mittelsteadt, and C. S. Gittleman, *J. Electrochem. Soc.*, **156**, B1440 (2009).
23. B. S. Pivovar and Y. S. Kim, *J. Electrochem. Soc.*, **154**, B739 (2007).
24. C. L. Gardner and A. V. Anantaraman, *J. Electroanal. Chem.*, **449**, 209 (1998).
25. K. M. Nouel and P. S. Fedkiw, *Electrochim. Acta*, **43**, 2381 (1998).
26. R. F. Silva, M. D. Francesco, and A. Pozio, *J. Power Sources*, **134**, 18 (2004).
27. M. Marechal, J.-L. Souquet, J. Guindet, and J.-Y. Sanchez, *Electrochem. Commun.*, **9**, 1023 (2007).
28. K. D. Kreuer, *Solid State Ionics*, **97**, 1 (1997).